applied sciences

MDPI

Article

Design and Research of a Three-Phase AC Magnetic Separator for Coal Desulfurization and Ash Reduction

Min Cao, Yan Chen *, Chunyan Ma and Qiang Liu

College of Electrical and Power Engineering, Taiyuan University of Technology, Taiyuan 030024, China; 15340650907@163.com (M.C.); tyutchyma@sina.com (C.M.); liuqiang3430@icloud.com (Q.L.)
* Correspondence: chenyan@tyut.edu.cn; Tel.: +86-135-9318-2148

Received: 25 March 2020; Accepted: 16 April 2020; Published: 21 April 2020

check for updates

Abstract: China's total coal consumption accounts for 50% of total energy consumption. However, every ton of coal in the process of production and use will bring huge losses to the environment. Desulfurization and ash removal of coal have been a continuous focus of researchers in various countries. The three-phase alternating current (AC) magnetic separator is a device for desulfurization and ash reduction of coal based on the principle of generating an alternating magnetic field generated by a three-phase flat linear motor. It is optimized by finite element analysis and its electromagnetic thrust is improved by 114% after optimization. Factors such as current size, magnetic particle size, and installation angle of the device are also analyzed. The simulation results show that the structure design of the three-phase AC magnetic separator is reasonable.

Keywords: magnetic separation desulfurization; three-phase AC magnetic separator; traveling wave magnetic field; electromagnetic force

---

1. Introduction

Coal dominates the primary energy consumption structure and will not change its dominant position in the energy mix in the next few years. However, due to the large amount of harmful substances emitted by coal burning, the deterioration of urban air quality and large-scale acid rain deposition have been caused. Therefore, actively analyzing the causes of coal-fired pollution and effectively removing sulfur from coal are of great significance for developing the economy, strengthening environmental protection, and managing severe acid rain.

At present, there are many methods for desulfurization and deashing of burning coal. According to the different desulfurization stages, the coal-fired desulfurization method can be divided into desulfurization and ash reduction before combustion, desulfurization and ash reduction in combustion, and finally desulfurization and ash reduction after combustion. According to the different media environments, it can be divided into dry desulfurization and wet desulfurization. Desulfurization before combustion is the source technology of clean coal. It can not only desulfurize, but also remove ash. It can also improve the efficiency of heat energy utilization, and its cost is much lower than that during and after combustion. In addition, considering that most coal-fired power plants use pulverized coal stoves, the boiler must be fired with dry powder if the wet desulfurization cannot be used to do the online sorting. Therefore, from the perspective of energy conservation and emission reduction, green and efficient, dry desulfurization and ash reduction before combustion is the best choice [1].

Brown [2] in the United States invented a frictional electric separator to remove pyrite and ash minerals from coal powder. The University of Western Ontario applied a dilute phase cyclone sorting machine to conduct coal sorting tests. The removal rate of pyrite was 47% [3]. Tao [4] developed a novel rotary turboelectric separator (RTS) with the advantage of a suitable range of particle sizes. Huang [5] conducted a triboelectric selection test of pulverized coal, and carried out single factor tests and orthogonal tests on air volume, voltage and particle size. The study found that there are optimal conditions for the effect of air volume and voltage on sorting. Song [6] used the surface modification method to pretreat the fine coal and used the rotary friction electric separator to separate it. The results show that the surface modification can significantly enhance the desulfurization and ash reduction effect of electrostatic separation with rotary friction. Zhang [7] applied the innovative rotary friction electroseparator to study the effects of the key operating parameters such as charger speed, separation voltage and airflow velocity on the ash reduction effect of rotary friction electroseparation for micropulverized coal. The above several desulfurization technologies belong to the frictional electrification technology. The main disadvantage of this method is the poor adaptability to different coal types. The sorting process is susceptible to air humidity and the upper limit of sorting is low.

The Eriez company in America developed Reium100 permanent magnet HGMS, which has a field strength of 0.6 T. The magnetic material is vertically placed, and the recovery rate of magnetic material is 96–99% [8]. In order to improve the efficiency of sorting, Ganzhou Nonferrous Metallurgy Research Institute developed a new generation of Slon HGMS [9] and Slon-1000 dry vibration HGMS [10], which has significantly improved the level of high-gradient magnetic separation technology. Johannes Lindner [11] developed a new equipment based on the high-gradient magnetic separator, which combines the high-gradient magnetic separation and sedimentation centrifugation, effectively overcoming the shortcomings of the traditional high-gradient magnetic separator that cannot be continuously separated. Cao [12] developed a new type of magnetic separator with the advantages of self-service, a dry process and permanent-magnet strength, as well as a strong vertical ring magnetic separator with a wide particle size. The industrial test results proved that the strong magnetic separation combination equipment can effectively expand the range of weak magnetic minerals. Zhang [13–15] used microwave energy to selectively heat pyrite in fine-grained coal to enhance its magnetic properties and achieve high-gradient magnetic separation. The research shows that by using a better second-order fitting model, the constraints of main influencing factors and the optimization indexes after response can be obtained. The above several desulfurization technologies belong to the high-gradient magnetic separation technology. The main disadvantage of this method are: when an electromagnet is used to generate a magnetic field, it consumes a large amount of energy and also increases the investment of the equipment and maintenance workload; when permanent magnet is used to generate a magnetic field, there are some disadvantages such as the imperfect magnetic structure, the "long beard" phenomenon in the magnetic system inside the discharge port and the magnetic working face, the mechanical inclusions in the sorting process, and the blockage of the magnetic medium.

In this paper, a three-phase AC magnetic separator for coal desulfurization and ash reduction is designed. The principle is that the three-phase flat linear motor can generate an alternating moving magnetic field. The separator has the characteristics of simple structure and a large separation amount, and there is no problem of blockage of the medium. The structure of the separator is optimized and the influence of different factors on electromagnetic force is analyzed by the finite element method.

This paper is organized as follows: after the introduction in Section 2, the basic structure and operation principle of three-phase AC magnetic separator are given, in Section 3, the structure of three-phase AC magnetic separator is optimized and its characteristics are analyzed, and in Section 4, conclusions are drawn.

2. Basic Structure and Operating Principle of the Three-Phase AC Magnetic Separator

2.1. Basic Structure of the Three-Phase AC Magnetic Separator

The three-phase AC magnetic separator utilizes the effect of the traveling wave magnetic field to discriminate the magnetic material. Under the action of the alternating magnetic field, the phenomenon of "flocculation" does not occur, the separation effect is good, the device structure is simple, and the separation amount is large.

The three-phase AC magnetic separator is designed based on the three-phase AC flat linear motor, which is composed of a 0.5 mm thick silicon steel sheet (DW465-50, Manufacturer name, city, state if US or Canada, country) with a stacking coefficient of 0.9. The basic structure is shown in Figure 1. The stator slot adopts an open slot, and the slot is filled with three-phase windings. The currents of the three-phase windings are equal in magnitude, but the difference between phases is 120 degrees. The stacking form is double-layered winding. The inner diameter of the enameled wire is 1 mm and the outer diameter is 1.062 mm. After the assembly is completed, the resin is sealed in the metal casing, and the surface of the device is covered with 3 mm wear-resistant ceramic. The three-phase AC magnetic separator is divided into two zones (unloading zone and adsorption zone), and three-phase symmetric windings are arranged under the wear-resistant ceramic in the adsorption zone. There is no winding under the wear-resistant ceramic in the unloading zone. The specific parameters of the three-phase AC magnetic separator are shown in Table 1.

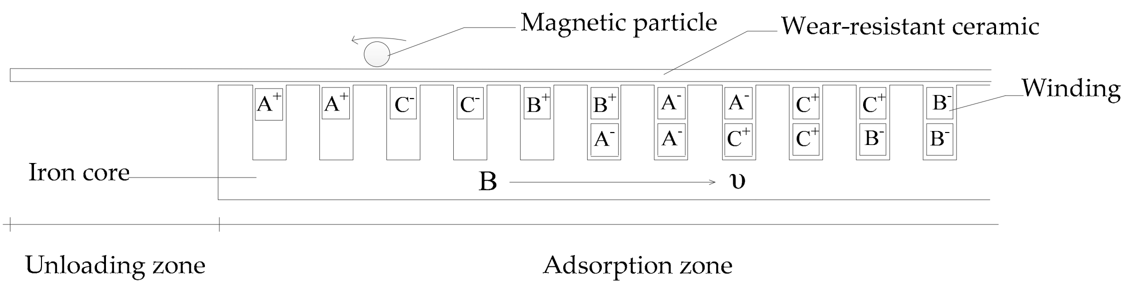

Figure 1. Schematic diagram of the three-phase alternating current (AC) magnetic separator.

Table 1. Three-phase alternating current (AC) magnetic separator parameters.

Parameter	Numerical Value	Parameter	Numerical Value
Total length L_s/mm	486	Total width W_s/mm	84
Total height H_s/mm	50	Slot width W_{ss}/mm	6.8
Slot depth H_{ss}/mm	35	Tooth width W_{sp}/mm	4.87

The Installation diagram of the three-phase AC magnetic separator is shown in Figure 2. The device is installed in the unloading end of the belt conveyor in the original pulverizing system of the power plant. The pulverized coal falls to the adsorption zone of the three-phase AC magnetic separator at a certain speed. Under the action of gravity, the pulverized coal and other diamagnetic substances follow the adsorption zone falls. The magnetic substance reaches the unloading zone from the adsorption zone under the action of the electromagnetic force generated by the three-phase traveling wave magnetic field, and there is no magnetic field in the unloading zone, so the magnetic material falls under the action of gravity. Therefore, the separation of diamagnetic material such as coal powder and magnetic material is realized. The finely ground coal is uniformly and loosely rolled on the surface of the desulfurization device to facilitate adsorption, and the magnetic field strength of the desulfurization device is greatly reduced, which is beneficial to energy conservation.

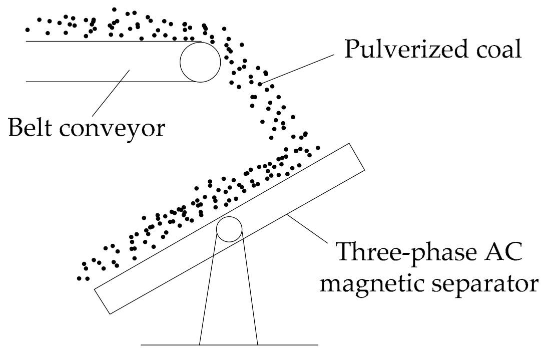

(**a**)Installation side view

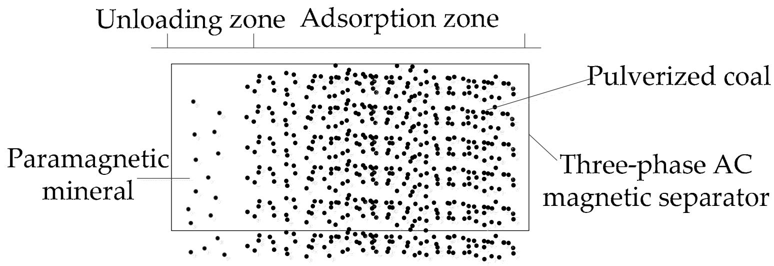

(**b**)Installation front view

Figure 2. Installation diagram of the three-phase ac magnetic separator.

2.2. The Working Principle of the Three-Phase AC Magnetic Separator

On the surface of the slotted core, a three-phase winding is embedded. When the winding is connected to the power supply, the three-phase current generates a traveling magnetic field that moves in a certain direction and at a certain speed on the surface of the core. The direction of the magnetic field motion is determined by the phase sequence of the current in the winding. Its moving speed is:

$$\nu = 2f\tau \tag{1}$$

in this formula, f is the power supply frequency and τ is the pole pitch of the winding.

As a result of this magnetic field, the magnetic particles attached to the surface roll to a certain extent, and the direction of the rolling is against the direction of the traveling wave magnetic field generated by the separator [16]. This phenomenon can be explained by Figure 3.

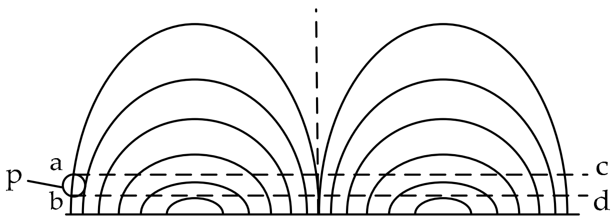

Figure 3. Rotating magnetic field component during the translation of a traveling wave magnetic field.

Take a card and open a small hole named P on the card to represent a certain magnetic particle placed on a surface of the separator. It is assumed that the moving direction of the traveling wave magnetic field is from right to left. According to the principle of relative motion, the magnetic field does not move, and the small hole P moves from left to right along the two lines ac and bd. In the small hole, it can be seen that the magnetic field passing through the small hole rotates clockwise, that is, the magnetic particles are in the traveling wave magnetic field. The magnetic field passing through the magnetic particles is a rotating magnetic field component, and the direction of rotation is opposite to the moving direction of the traveling magnetic field. Under the action of this magnetic field, the magnetic particles will produce a clockwise torque that causes the particles to roll against the direction of the traveling magnetic field on the surface of the separator. This is the working principle of a three-phase AC magnetic separator. The effect of this magnetic field on the particles is called the "rack–gear" effect [17].

2.3. Force Analysis of Magnetic Particles on the Magnetic Separator

The magnetic particles are subjected to three forces during the sorting process, namely gravity F_G, fluid resistance F_D and magnetic force F_m, wherein the gravity F_G of the magnetic particles is:

$$F_G = \frac{\pi}{6} d^3 \rho g \tag{2}$$

in this formula, ρ is the density of the object; g is the acceleration of gravity; d is material diameter.

The fluid resistance F_D acting on paramagnetic particles is:

$$F_D = 3\pi\eta d v \tag{3}$$

in this formula, η is the viscosity of the fluid; v is the flow rate; d is the diameter of the material.

In the traveling wave magnetic field, the magnetic particles are subjected to two kinds of magnetic forces: magnetic suction and hysteresis torque. The suction force F is:

$$F = V \frac{(\mu_r - 1)H_0}{[4\pi + D(\mu_r - 1)]} \mathrm{grad} B_0 \tag{4}$$

in this formula, V is the volume of the magnetic particles; μ_r is the relative magnetic permeability; H_0 is the external magnetic field strength; D is the demagnetization factor, which is related to the shape of the magnetic particles, $D = 4\pi/3$ to the sphere or square; B_0 is the external magnetic field magnetic induction.

The suction force F_m per unit mass of magnetic particles is:

$$F_m = X_m H_0 \mathrm{grad} B_0 \tag{5}$$

in this formula, X_m is the specific magnetic susceptibility of the magnetic particles; H_0 is the external magnetic field strength; and B_0 is the external magnetic field magnetic induction.

As shown in Figure 4a, the magnetic particles are magnetized by the magnetic field at the surface of the separator, causing the particles to induce a corresponding polarity in the direction of the magnetic field. As shown in Figure 4b, after a certain period of time, the magnetic field is rotated by a certain angle. Due to the hysteresis effect of the magnetic particle material, the polarity is too late to change, so the magnetic particles generate a counterclockwise torque and cause the magnetic particles to roll in a counterclockwise direction on the separator surface.

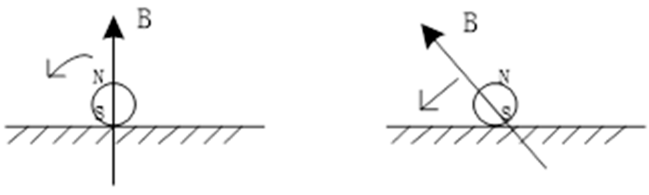

(**a**) (**b**)

Figure 4. Hysteresis moments of magnetic particles on the surface of the separator. (**a**) Polarity of magnetic particles before magnetic field rotation, (**b**) Polarity of magnetic particles after rotation of magnetic field.

The magnitude of this torque T can be expressed by the following formula:

$$T = V\frac{2\pi\mu_r {H_0}^2}{4\pi + D(\mu_r - 1)}\sin\gamma_0 \tag{6}$$

in the formula, γ_0 is the hysteresis angle, which is related to the material properties.

The hysteresis torque per unit mass is:

$$T_m = V\frac{2\pi\mu_r {H_0}^2}{\rho[4\pi + D(\mu_r - 1)]^2}\sin\gamma_0 \tag{7}$$

When the magnetic particles fall on the surface of the magnetic separator, due to the magnetic attraction force, the magnetic particles are pulled toward the surface of the separator. The hysteresis torque generated by the action of the rotational component in the magnetic field causes the magnetic particles rolling along the surface of the separator to overcome the fluid resistance F_D as well as the friction generated by the component of gravity F_G. The nonmagnetic material falls under the action of gravity, thus separating the magnetic material from the nonmagnetic material.

3. Structural Optimization and Characteristic Analysis of the Three-Phase AC Magnetic Separator

Using Ansys Maxwell (19, ANSYS, Pittsburghcity, Commonwealth of Pennsylvaniastate, US, 2018), the magnetism of magnetic particles is pyrite magnetism heated by microwave energy, and the three-phase AC magnetic separator is optimized in the transient field. Based on this, the finite element analysis of the influence of various factors on the electromagnetic thrust is carried out.

3.1. Structural Optimization of the Three-Phase AC Magnetic Separator

3.1.1. Tooth and Slot Size Optimization of the Three-Phase AC Magnetic Separator

In Ansys Maxwell (19, ANSYS, Pittsburghcity, Commonwealth of Pennsylvaniastate, US, 2018), based on the original data in the second section, the single-sided three-phase AC magnetic separator model is established and simulated. When the three-phase current is 5A, the electromagnetic thrust is as shown in Figure 5.

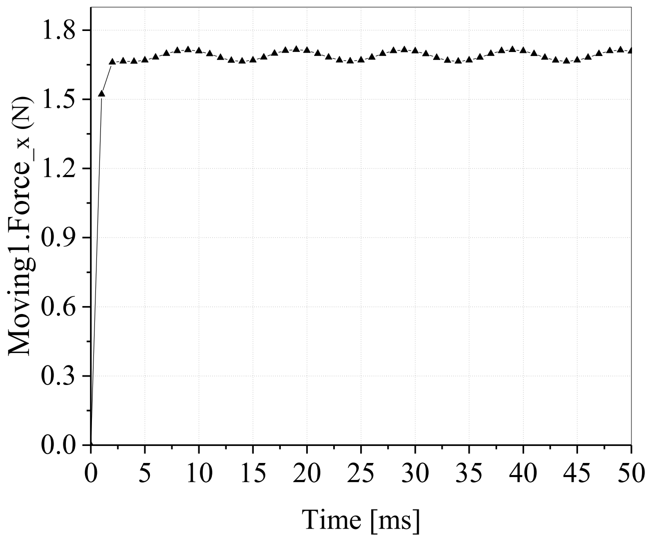

Figure 5. The electromagnetic thrust generated by the original model.

The mover of the three-phase AC magnetic separator is made up of magnetic particles, which is very different from the mover of the three-phase AC linear motor. As can be seen from Figure 5, the generated thrust is small, so it is necessary to optimize the structure. Since the leakage magnetic flux directly affects the leakage reactance, it restricts the electromagnetic thrust. The parameters affecting the leakage flux of the groove are mainly the slot depth (Hss) and the slot width (Wss), and as such Hss and Wss are simultaneously optimized.

Using the Ansys Maxwell (19, ANSYS, Pittsburghcity, Commonwealth of Pennsylvaniastate, US, 2018), the slot depth and the slot width are optimized variables. The values of the variables are Wss ∈ [4,10] mm, Hss ∈ [20,40] mm. Genetic algorithm is used to optimize the thrust. From Figure 6, it can be seen that the genetic iteration has a total of more than 700 genetic iterations, and the electromagnetic thrust fluctuates within a large range of 0.9 N to 3.56 N. Therefore, it is very important to optimize the slot parameters when designing a three-phase ac magnetic separator. Table 2 lists the data of the thrust from large to small. It can be seen that the electromagnetic thrust is the largest when Hss = 20.22 mm and Wss = 9.43 mm. Thus, Wss = 9.43 mm, Hss =20.22 mm is determined without changing the pitch.

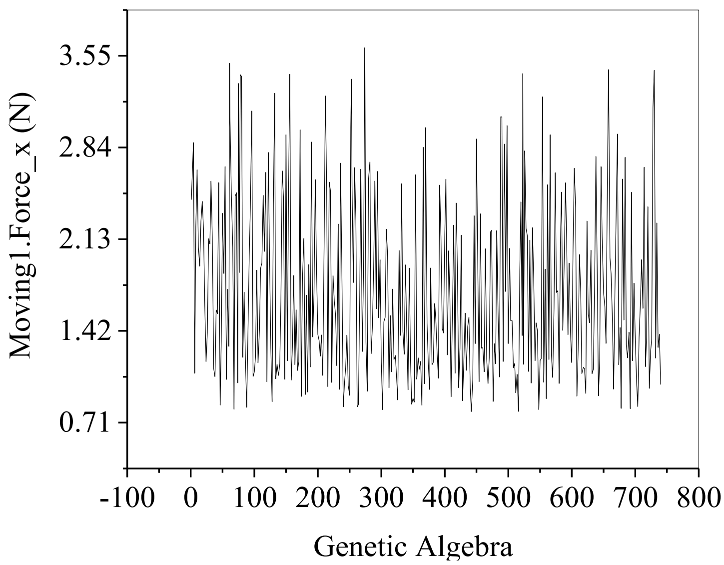

Figure 6. Genetic algorithm optimization.

Table 2. Specific values of genetic algorithm optimization.

Slot Width W_{ss}/mm	Slot Depth H_{ss}/mm	Electromagnetic Thrust/N
9.43	20.22	3.56
9.27	23.74	3.53
9.57	20.17	3.52
9.21	22.12	3.51
9.88	23.75	3.54

When the three-phase current is 5A, the optimized electromagnetic thrust is shown in Figure 7. After optimization, dates are shown in Table 3, the electromagnetic thrust is increased by 114%, and the optimization effect is remarkable.

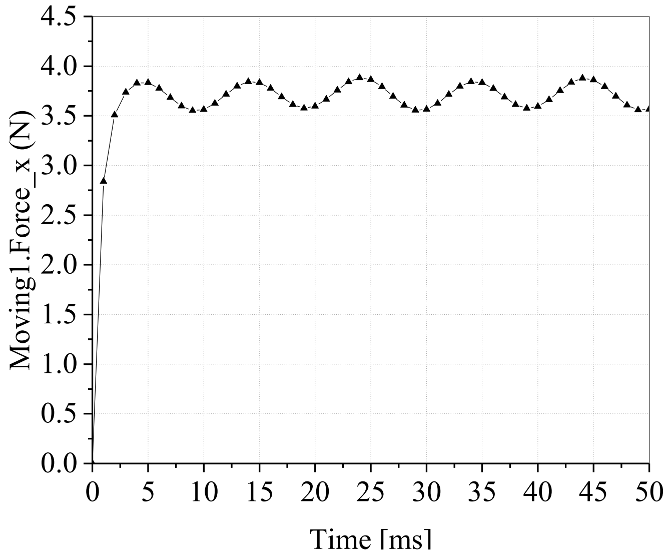

Figure 7. The thrust waveform generated after finite element optimization.

Table 3. Before and after optimization.

	Original Parameter	Optimized Simultaneously	Compared
Slot width W_{ss}/mm	6.8	9.43	-
Slot depth H_{ss}/mm	35	20.22	-
Electromagnetic thrust F_x/N	1.66	3.56	114%
Electromagnetic suction F_y/N	0.35	0.67	91%

3.1.2. Comparative Analysis of a Single-Sided and Double-Sided Three-Phase AC Magnetic Separator

Using the optimized tooth and slot size in Section 3.1.1, the double-sided three-phase AC magnetic separator model is established and simulated in ANSYS Maxwell (19, ANSYS, Pittsburgh, Commonwealth of Pennsylvania, US, 2018). The electromagnetic thrust is shown in Figure 8.

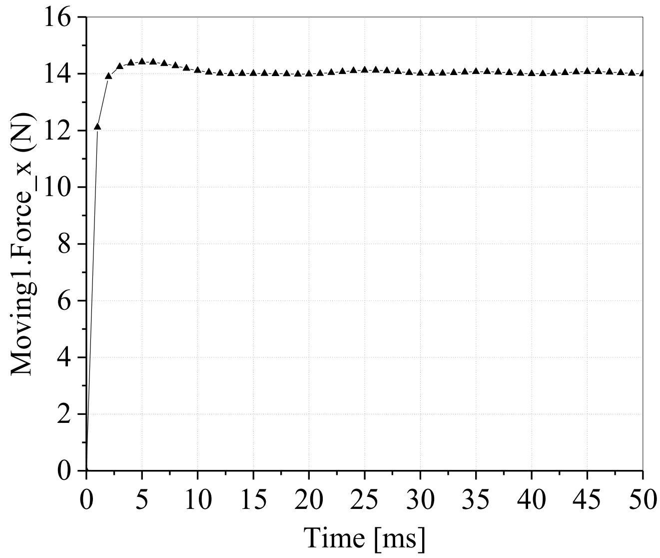

Figure 8. The electromagnetic thrust generated by the double-sided model.

Comparing the thrust generated by the simulation of single-sided and double-sided three-phase AC magnetic separators, it is found that the electromagnetic thrust generated by the double-sided structure is 3.9 times that of the single-sided structure. Therefore, when the double-sided structure is used, the desulfurization effect of the three-phase AC magnetic separator is better.

3.2. Magnetic Saturation Analysis

Magnetic saturation seriously affects the performance of the three-phase AC magnetic separator. When it is in magnetic saturation, the magnetic pull force will not increase linearly as the winding current increases. Therefore, it is necessary to avoid the saturation phenomenon when designing the three-phase AC magnetic separator. The magnetization curve of the silicon steel sheet is shown in Figure 9. As can be seen from the figure, when the magnetic density reaches saturation, the magnetic density value is 17,500 Gauss.

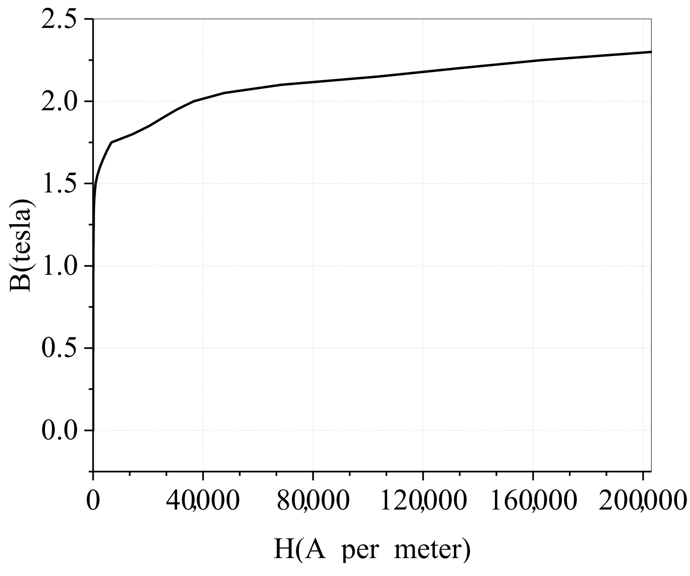

Figure 9. Silicon steel sheet B–H curve.

When the three-phase windings of A, B, and C are connected with 5A, 10A and 12.5A currents, the magnetic density distribution of the three-phase AC magnetic separator is as shown in Figure 10.

It can be seen from the analysis in Figure 10 that when the current value increases, the magnetic density value increases gradually, and when the current value is less than 12.5A, the maximum magnetic density of the three-phase AC magnetic separator is lower than the saturation magnetic density of the silicon steel sheet, which can be considered as a linear model.

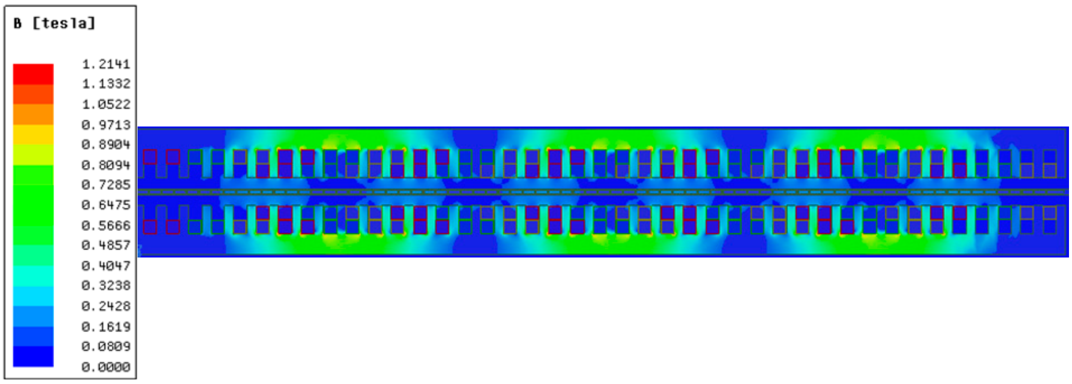

(**a**) 5A

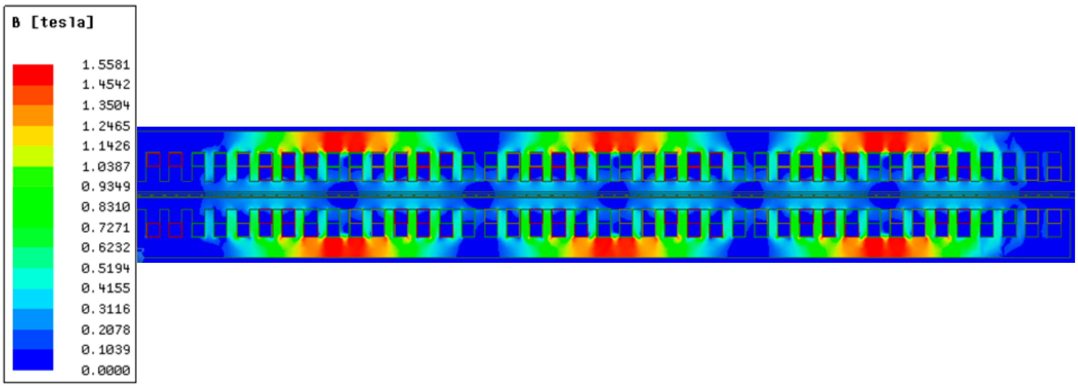

(**b**) 10A

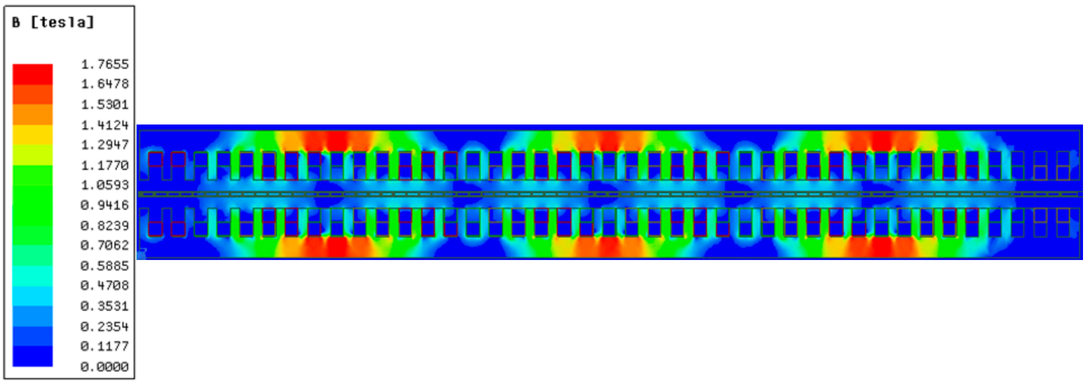

(**c**) 12.5A

Figure 10. Magnetic density distribution at different currents.

3.3. Effects of Current on Electromagnetic Thrust

When the magnetic particle size is 0.15 mm and the three phases A, B, and C are connected to 5A, 6A, 7A, 8A and 9A, the electromagnetic thrust generated by the three-phase AC magnetic separator is as shown in Figure 11. As can be seen from Figure 11, as the current increases, the electromagnetic thrust increases, and the electromagnetic thrust generated when the current is 9A is 3 times that of the electromagnetic thrust generated when the current is 5A.

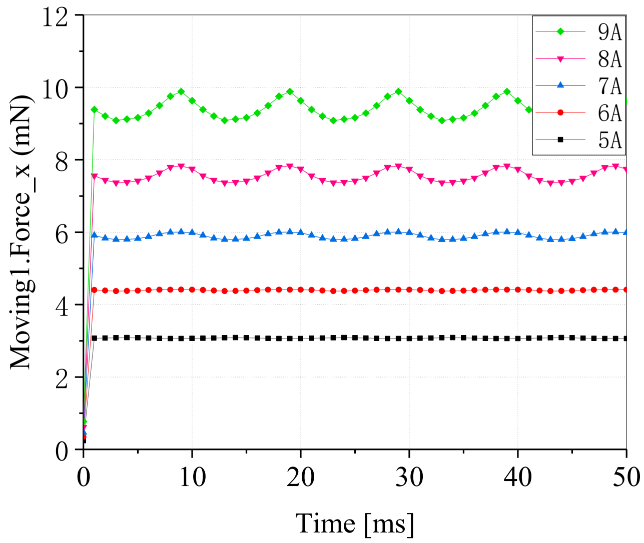

Figure 11. Electromagnetic force generated at different currents.

When the three-phase AC magnetic separator is energized with 5A and the magnetic particle size is 0.15 mm, the specific values of the various forces of the magnetic particles are shown in Table 4. The friction coefficient of the wear-resistant ceramic on the surface of the three-phase AC magnetic separator is 0.2, and the fluid resistance on the magnetic particles is obtained by the formula (3) $F_D = 3\pi\eta dv$, where in $\eta = 17.6 \times 10^{-6}$ pa·s. As can be seen from Table 4, when the magnetic particle size is 0.15 mm, the acceleration is 4.4555 m·s $^{-2}$, that is, the three-phase AC magnetic separator can quickly transport it to the unloading zone. Therefore, when the current is greater than 5A, the magnetic particles must be transported to the unloading zone at a faster speed.

Table 4. Various forces acting on magnetic particles.

The Size of Granule	The Force the Particle Receives					
	Electromagnetic Thrust/N	Electromagnetic Pull/N	Friction /N	Resistance F_D/N	Joint Force /N	Acceleration /m·s^{-2}
0.15 mm	3.0447×10^{-3}	1.1914×10^{-4}	9.5981×10^{-4}	1.0122×10^{-7}	2.0848×10^{-3}	4.4555

It can be seen from the above analysis that, according to the actual situation, the moving speed of the magnetic particles can be changed by adjusting the magnitude of the current to achieve the purpose of magnetic desulfurization.

3.4. Effects of Particle Size of Magnetic Particles

When the three phases A, B, and C are connected to 5A, and the magnetic particle size is 0.074 mm, 0.1 mm and 0.15 mm respectively, the electromagnetic thrust generated is as shown in Figure 12. As can be seen from Figure 12, when the particle size of the magnetic particles increases, the electromagnetic thrust tends to increase. As the particle size of the magnetic particles increases, the friction generated by its own gravity also increases. Therefore, in order to judge whether the magnetic particles can be quickly transported to the unloading zone when the current is 5A, specific stress analysis of the magnetic particles is required.

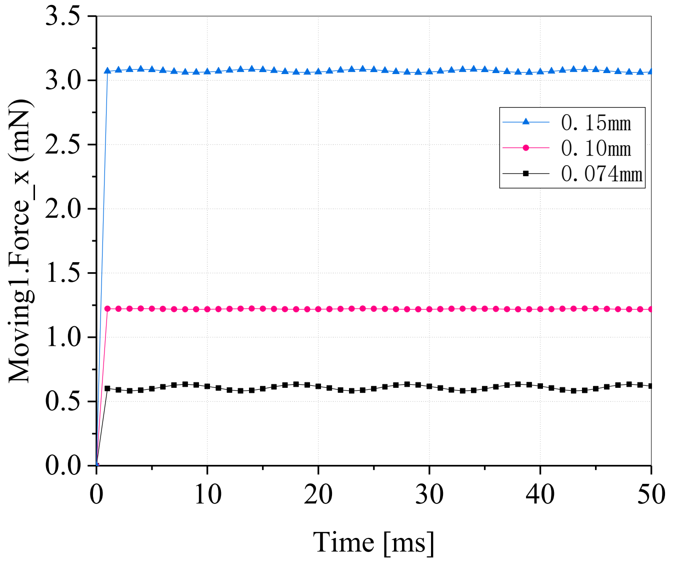

Figure 12. Electromagnetic force generated at different particle diameters.

The friction coefficient of the wear-resistant ceramic on the surface of the three-phase AC magnetic separator is 0.2, and the fluid resistance on the magnetic particles is obtained by the formula (3) $F_D = 3\pi\eta dv$, where in $\eta = 17.6 \times 10^{-6}$ pa·s. The specific values of the various forces of the magnetic particles are shown in Table 5.

Table 5. Various forces acting on magnetic particles.

The Size of Particle	Electromagnetic Thrust/N	Electromagnetic Pull/N	Friction/N	Resistance F_D/N	Joint Force /N	Acceleration /m·s^{-2}
0.074 mm	0.6024×10^{-3}	4.6528×10^{-5}	1.2167×10^{-4}	4.9914×10^{-8}	4.8068×10^{-4}	8.5561
0.10 mm	1.2075×10^{-3}	1.4152×10^{-4}	3.0558×10^{-4}	6.7481×10^{-8}	9.0185×10^{-4}	6.5049
0.15 mm	3.0447×10^{-3}	1.1914×10^{-4}	9.5981×10^{-4}	1.0122×10^{-7}	2.0848×10^{-3}	4.4555

It can be seen from Table 5 that under the condition that the three-phase current is 5A, and the magnetic particle size is 0.074 mm, 0.1 mm, and 0.15 mm, the three-phase AC magnetic separator can transport the magnetic particles to the unloading area.

3.5. Impacts of Mounting Tilt Angle

In the alternating moving magnetic field, when the electromagnetic force of the magnetic particles is greater than the competitiveness of gravity and fluid resistance, the purpose of magnetic desulfurization can be achieved [18]. The tangential force (parallel to the surface of the three-phase AC magnetic separator) and radial force (perpendicular to the surface of the three-phase AC magnetic separator) generated by the gravity of magnetic particles gravity along the surface of the three-phase alternating current magnetic separator are closely related to the installation tilt angle of the device. Next, the influence of the installation angle of the device on the resultant force of the magnetic particles is analyzed.

When the installation angles θ of the three-phase AC magnetic separator are 10°, 30°, and 60°, the tangential force and radial force caused by the gravity of magnetic particles of different particle sizes are shown in Tables 6 and 7, respectively.

Table 6. Tangential forces(N) at different installation angles and different particle sizes.

Installation Angle	The Size of Particle		
	0.074 mm	**0.10 mm**	**0.15 mm**
10°	1.71134×10^{-6}	4.2232×10^{-6}	1.4253×10^{-5}
30°	5.13396×10^{-6}	1.2669×10^{-5}	4.2759×10^{-5}
60°	1.02675×10^{-5}	2.5338×10^{-5}	8.5515×10^{-5}

Table 7. Radial forces(N) with different mounting angles and different particle sizes.

Installation Angle	The Size of Particle		
	0.074 mm	**0.10 mm**	**0.15 mm**
10°	5.6180×10^{-4}	1.3864×10^{-3}	4.6791×10^{-3}
30°	5.6178×10^{-4}	1.3863×10^{-3}	4.6789×10^{-3}
60°	5.6171×10^{-4}	1.3863×10^{-3}	4.6783×10^{-3}

When the current is 5A, the force analysis of the magnetic particles on the three-phase AC magnetic separator is shown in Figure 13. The friction coefficient of the wear-resistant ceramic on the surface of the three-phase AC magnetic separator is 0.2, and the fluid resistance on the magnetic particles is obtained by the formula (3) $F_D = 3\pi\eta dv$, wherein $\eta = 17.6 \times 10^{-6}$ pa·s. When the installation angle of the device is 10°, 30°, and 60°, the specific values of the various forces applied to the magnetic particles are shown in Table 8.

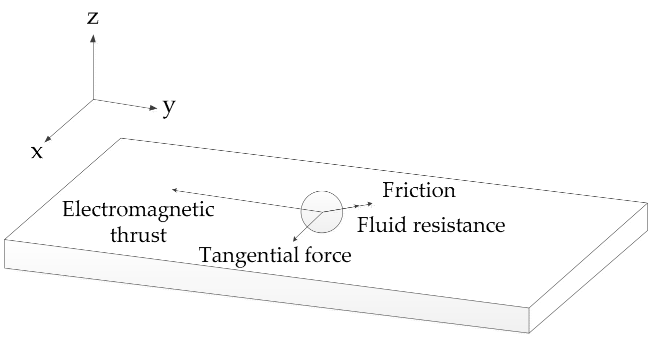

Figure 13. Force analysis of magnetic particles.

Table 8. Various forces acting on magnetic particles.

The Size of Particle		The Force on the Particle					
		Electromagnetic Thrust/N	**Electromagnetic Pull/N**	**Friction/N**	**Fluid Resistance F_D/N**	**Resultant Force/N**	**Acceleration/ m·s^{-2}**
0.074 mm	θ = 10°	0.6024×10^{-3}	4.6528×10^{-5}	1.2167×10^{-4}	4.9914×10^{-8}	4.8068×10^{-4}	8.5561
	θ = 30°			1.2166×10^{-4}		4.8071×10^{-4}	8.5566
	θ = 60°			1.2165×10^{-4}		4.8079×10^{-4}	8.5580
0.10 mm	θ = 10°	1.2075×10^{-3}	1.4152×10^{-4}	3.0558×10^{-4}	6.7481×10^{-8}	9.0186×10^{-4}	6.5051
	θ = 30°			3.0556×10^{-4}		9.0194×10^{-4}	6.5056
	θ = 60°			3.0552×10^{-4}		9.0218×10^{-4}	6.5074
0.15 mm	θ = 10°	3.0447×10^{-3}	1.1914×10^{-4}	9.5965×10^{-4}	1.0122×10^{-7}	2.0850×10^{-3}	4.4560
	θ = 30°			9.5961×10^{-4}		2.0853×10^{-3}	4.4566
	θ = 60°			9.5949×10^{-4}		2.0863×10^{-3}	4.4588

It can be known from Table 8 that, due to the large electromagnetic force received by the magnetic particles, the effect of gravity is small, so when the installation tilt angle of the three-phase AC magnetic separator increases, the acceleration change of the magnetic particles is not obvious. The diamagnetic particles are not affected by electromagnetic forces, so their gravity will affect the speed of their fall.

Therefore, in the sorting process, the falling speed of the diamagnetic particles can be adjusted by adjusting the inclination angle of the three-phase AC magnetic separator.

4. Conclusions

In this paper, a three-phase AC magnetic separator for desulfurization and ash reduction of coal is designed. The structure size of the three-phase AC magnetic separator and the winding mode are determined. The structure optimization and magnetic saturation analysis of three phase AC magnetic separator are carried out by finite element analysis, and the influence of current, size of magnetic particle and installation angle on electromagnetic thrust is analyzed. Simulation results show:

(1) After structural optimization, the electromagnetic thrust of the three-phase AC magnetic separator is 8 times that of the original;
(2) When the three-phase current is less than 12.5A, the magnetic density of the three-phase AC magnetic separator is lower than the saturation magnetic density of the silicon steel sheet, which can be considered as a linear model;
(3) As the current increases, the electromagnetic force tends to increase. Therefore, in actual situations, when the magnetic particles are weakly magnetic, a larger current can be used; when the magnetic particles are strongly magnetic, a smaller current can be used, so as to achieve the effect of energy saving. The movement speed of the magnetic particles can be changed by adjusting the magnitude of the current to achieve the purpose of magnetic desulfurization;
(4) When the three-phase current is 5A, the larger the particle size of the magnetic particles, the smaller the acceleration;
(5) As the magnetic particle size is small, the electromagnetic force is large, and the influence of gravity is small, the acceleration of the magnetic particle does not change obviously when the installation angle of the three-phase AC magnetic separator increases. Therefore, in the sorting process, the falling speed of the diamagnetic particles can be adjusted by altering the inclination angle of the three-phase AC magnetic separator.

Author Contributions: Conceptualization, Y.C.; investigation, M.C.; methodology, C.M.; software, Q.L.; validation, C.M.; writing original draft, Y.C. All authors have read and agreed to the published version of the manuscript.

Funding: This research is supported by the Natural Science Foundation of Shanxi Province (201701D121127), the Key Research and Development (R&D) Projects of Shanxi Province (201803D221028-2) and the Key Research and Development (R&D) Projects of Shanxi Province (201903D121015).

Acknowledgments: Xiaomin Chang provided valuable advice on the study idea and write-up. Thanks also go to Wentao Wu, Yanzhao Hao, Rui Chen and Jinmeng Wu for their assistance during the research.

Conflicts of Interest: The authors declare no conflict of interest. The founding sponsors had no role in the design of the study; in the collection, analyses, or interpretation of data; in the writing of the manuscript, and in the decision to publish the results.

References

1. Chen, Y.; Cao, M.; Ma, C. Review of Coal-fired Electrification and Magnetic Separation Desulfurization Technology. *Appl. Sci.* **2019**, *9*, 1158. [CrossRef]
2. Brown, D.K. Electrostatic Pyrite Ash and Toxic Mineral Separator. U.S. Patent 5637122, 10 June 1997.
3. Jiao, H.; Cui, J.; Chen, Q. Review on dry desulphurization and ash reduction technology of pulverized coal before combustion. *Coal Qual. Technol.* **2007**, *2*, 43–45,47. [CrossRef]
4. Tao, D.; Sobhy, A.; Li, Q.; Zhao, Y. Dry cleaning of pulverized coal using a novel rotary triboelectrostatic separator (RTS). *Int. J. Coal Prep. Util.* **2011**, *31*, 187–202. [CrossRef]
5. Huang, G.; Luo, S.; Zhou, Y.; Ma, Y.; Yi, Y. Triboelectric separation of pulverized coal. *Coal Technol.* **2015**, *34*, 315–317. [CrossRef]
6. Song, A.; Tao, Y.; Xian, Y.; Zhang, X.; Ding, Q. Experimental study on desulfurization and ash reduction of micro pulverized coal by surface modification and enhanced rotary friction electric separation. *China Coal* **2015**, *12*, 79–85. [CrossRef]

7. Zhang, W.C.; Tao, Y.; Song, A.; Xian, Y.S.; Man, Z.P.; Xue, Y.W. Experimental study on dust reduction by rotating friction electric separation of micro-pulverized coal. *Coal Sci. Technol.* **2017**, *45*, 196–200. [CrossRef]
8. Feng, D.; Sun, Z. The present situation and Progress of permanent Magnet Separator. *Ore Dress. Foreign Metals* **1992**, *12*, 1–5.
9. Xiong, D.; Liu, J. New Progress of Slon pulsation and Vibration High gradient Magnetic Separator. *Met. Mine* **2006**, *361*, 4–7. [CrossRef]
10. Liu, X.; Chen, J. Development of a new Slon- 1000 dry vibration high gradient magnetic separator. *Non Metal. Min.* **2006**, *29*, 32–34. [CrossRef]
11. Lindner, J.; Nirschl, H. A hybrid method for combining High-Gradient Magnetic Separation and centrifugation for a continuous process. *Sep. Purif. Technol.* **2014**, *131*, 27–34. [CrossRef]
12. Cao, Z.; Li, W.; Qian, S. Development and Application of New Strong Magnetic Separation Combination Equipment. *Metal Mine* **2016**, *12*, 122–125. [CrossRef]
13. Zhang, B.; Zhao, Y.; Zhou, C.; Duan, C. Fine Coal Desulfurization by Magnetic Separation and the Behavior of Sulfur Component Response in Microwave Energy Pretreatment. *Energy Fuels* **2015**, *29*, 1243–1248. [CrossRef]
14. Zhang, B.; Fan, X.; Zhao, Y.; Cai, L. Desulfurization of microwave pretreated fine coal by magnetic separation. *Part. Sci. Technol.* **2018**, *36*, 600–608. [CrossRef]
15. Zhang, B.; Zhu, G.; Sun, Z.; Yan, G.; Yao, H. Fine coal desulfurization and modeling based on high-gradient magnetic separation by microwave energy. *Fuel* **2018**, *217*, 434–443. [CrossRef]
16. Ye, Y. *Principle and Application of Linear Motor*; China Machine Press: Beijing, China, 2000; ISBN 7-111-08050-5.
17. Gu, J.; Chen, W.; Lei, J. Three-phase AC magnetic separator. *Metall. Equip.* **1989**, *4*, 14–17.
18. Zhang, Y.; Shi, C.; Ma, J.; Zhang, Q. *Pulverized Coal Magnetic Separation Purification Technology*; Chemical Industry Press: Beijing, China, 2013; ISBN 7122165957.